

**BIOLOGY
LETTERS**

**The Thin(ning) Green Line? Investigating Changes in
Kenya's Seagrass Coverage**

Journal:	<i>Biology Letters</i>
Manuscript ID	RSBL-2018-0227.R2
Article Type:	Research
Date Submitted by the Author:	n/a
Complete List of Authors:	Harcourt, William ; Edinburgh Napier University , School of Applied Sciences Briers, Robert; Napier University, School of Applied Sciences Huxham, Mark; Edinburgh Napier University, School of Applied Sciences
Subject:	Environmental Science < BIOLOGY, Ecology < BIOLOGY
Categories:	Global Change Biology
Keywords:	mapping, seagrass, Kenya, blue carbon

SCHOLARONE™
Manuscripts

21 Abstract

22 Knowledge of seagrass distribution is limited to a few well-studied sites and poor where resources
23 are scant (e.g. Africa), hence global estimates of seagrass carbon storage are inaccurate. Here, we
24 analysed freely available Sentinel-2 and Landsat imagery to quantify contemporary coverage and
25 change in seagrass between 1986 and 2016 on Kenya's coast. Using field surveys and independent
26 estimates of historical seagrass, we estimate total cover of Kenya's seagrass to be $317.1 \pm 27.2 \text{ km}^2$,
27 following losses of $0.85\% \text{ yr}^{-1}$ since 1986. Losses increased from $0.29\% \text{ yr}^{-1}$ in 2000 to $1.59\% \text{ yr}^{-1}$ in
28 2016, releasing up to 2.17 Tg carbon since 1986. Anecdotal evidence suggests fishing pressure is an
29 important cause of loss and is likely to intensify in the near future. If these results are representative
30 for Africa, global estimates of seagrass extent and loss need reconsidering.

31 Keywords

32 Seagrass, Mapping, Kenya, Blue Carbon

33

34

35

36

37

38

39

40

41

42 Introduction

43 Despite the increasing sophistication of Blue Carbon science, some basic information remains
44 imprecise. Prominent among this is the regional extent of seagrass habitats, which is essential in
45 determining seagrass carbon (C) stocks and flows. Knowledge of seagrass coverage is globally
46 variable; for example, the USA is well studied, representing 130 of the 215 sites detailed in a review
47 of global trends [1]. By contrast, Africa remains poorly mapped, with paltry information on seagrass
48 extent, ecology and C stocks [2]. Given the large areas and high C concentrations that may be
49 present in Africa and other poorly researched tropical regions [3], current global estimates may be
50 very inaccurate.

51 Blue Carbon habitats are globally threatened; indeed the estimated $7\% \text{ yr}^{-1}$ loss of seagrass may be
52 the worst trend for any global habitat [1]. Having good data on rates of decline and drivers of loss
53 are essential. However, problems involved in mapping current seagrass coverage are magnified
54 when estimating trends. Historical data are of widely varying accuracy with no information at all for
55 many sites before the late 1970s and the first Landsat satellite images. The low radiometric
56 resolution and spectral sensitivity of Landsat 1-5 imagery impedes seagrass mapping, particularly for
57 sub-tidal areas. Whilst the advent of high resolution, freely available imagery represents enormous
58 progress, logistical and technical challenges remain in using these for seagrass monitoring and in
59 deriving comparisons between current and historical data.

60 Here, we estimate current and historical seagrass coverage in Kenya. We produce the first national
61 analysis of seagrass cover change that begins to address the large gap in knowledge from the African
62 continent and allows comparison with better-known areas of the world. In addition, we aim to
63 illustrate an approach of relevance to seagrass mapping in general. Our objectives were:

- 64 1) To map the contemporary coverage of seagrass on Kenya's coast using the highest
65 resolution freely available imagery.

66 2) To reveal rates of change over the past 30 years and examine the implications for C storage
67 and loss.

68 Methods

69 Seagrass coverage for 2016 was mapped using Landsat 8 (LC8) and Sentinel-2 (S2). Coverage in 2000
70 and 1986 were estimated using Landsat 7 (LE7) and Landsat 5 Thematic Mapper (TM5), respectively.
71 Sen2Cor and LEDAPS were used to convert S2 and Landsat imagery, to Bottom-of-Atmosphere (BOA)
72 reflectance and to remove clouds. Images were projected to WGS 1984 UTM zone 37 South
73 coordinate system. Images were paired to represent high and low tide conditions. Water was
74 separated from land by thresholding Normalised Difference Water Index (NDWI) values, and
75 differenced between image pairs to extract image specific emergent and submerged zones.
76 Correlating NIR reflectance with the visible wavelengths in deep water allowed us to correct for the
77 specular reflection of light from the ocean surface [4].

78 The emergent region was classified using the ISODATA unsupervised classification method due to
79 the absence of spatially distributed field data. Resultant classes were merged by assigning a
80 similarity threshold to a dendrogram, computed from individual class attributes. Groups of pixels
81 (~10-20) were assessed, and the presence of seagrass determined by comparing reflectance profiles
82 to ground-based spectral profiles [5], examining the original image, using local field knowledge, and
83 reviewing all relevant literature and official reports on Kenyan seagrass.

84 For the submerged regions, we computed a relative water depth grid (WD_{rel}), based on the ratio
85 between the linearized blue (R_{Blue}) and green (R_{Green}) bands in each image [6], and isolated
86 anomalies removed by using Segment Mean Shift within ArcGIS 10.5. The transition to deep water is
87 signalled by a sudden drop in WD_{rel} , and a threshold used to exclude these pixels. Discrete zones of
88 WD_{rel} were extracted using a quantile interval method, classified using the same approach as
89 above, and corrected for the presence of coral by thresholding the ratio of the red to green band

90 across all depths [7]. Such hierarchical classification schemes circumvent the effects of water depth
91 changes to benthic reflectance [8].

92 Point measurements of seagrass presence and absence were recorded from Gazi Bay (432) and
93 Vanga Bay (27) (Fig. 1) using a GoPro Hero 4 and a stratified random sampling technique in 2017 (see
94 [9] for more information). Overall Accuracy (OA) was derived from a confusion matrix between the
95 field data and S2 derived seagrass coverage. The accuracy of LT5 (1986), LE7 (2000), and LC8 (2016)
96 maps were determined by calculating two independent estimates for each time period, from
97 separate image sets overlapping in time and space. A confusion matrix was derived from this
98 overlap, and OA computed (Landsat image overlap method).

99 We mapped seagrass coverage for a single Landsat path and row scene across four dates between
100 2015 and 2016 to assess intra-annual and short-term variability and found it to be minimal [9].

101 We estimated total organic carbon (C_{org}) stored within Kenya's seagrass using the following
102 equation:

$$Total C_{org} = A \times (Biomass C_{org} + Sediment C_{org})$$

103 where A is total seagrass cover. Regional estimates of biomass C_{org} and sediment C_{org} for
104 seagrasses in Gazi bay (Fig. 1) are $585 \pm 43 \text{ Mg C km}^{-2}$ and $23,557 \pm 2,437 \text{ Mg C km}^{-2}$ [3], respectively.
105 In comparison, global seagrass biomass C_{org} and sediment C_{org} are estimated to be $251 \pm 48 \text{ Mg C}$
106 km^{-2} and $16,560 \text{ Mg C km}^{-2}$, respectively [10]. Destruction of seagrass leads to loss of biomass C_{org} ,
107 whereas sediment C_{org} may stabilise or be rapidly lost [11]. Here we estimate maximum feasible C
108 loss by assuming sediment C_{org} in the top 1 m reverts to $4,967 \text{ Mg C km}^{-2}$ (the average value for
109 unvegetated sediment reported in [3]) following seagrass loss.

110 Results

111 Seagrass extends along the coast of Kenya, with the exception of the Tana River delta, probably due
112 to high turbidity (Fig. 1). Total 2016 seagrass coverage was estimated as $317.1 \pm 27.2 \text{ km}^2$ (LC8) and
113 $308.4 \pm 40.8 \text{ km}^2$ (S2) (Fig. 2). Of this, 62% occurs north of Malindi ('northern Kenya'), particularly the
114 Lamu Archipelago (Fig. 1). Southern Kenyan seagrasses occupy the reef crests, inlets and lagoons
115 from Vanga Bay to Malindi (Fig. 1). Emergent seagrass (area exposed at the time of image
116 acquisition) made up 64.2% of the total seagrass cover.

117 Kenya's seagrass declined by $0.85\% \text{ yr}^{-1}$ since 1986 (Fig. 2), accelerating from $0.29\% \text{ yr}^{-1}$ (1986-2000)
118 to $1.59\% \text{ yr}^{-1}$ (2000-2016). Losses in the north were consistent between 1986 and 2016 ($1.02\% \text{ yr}^{-1}$),
119 whereas initial increases between 1986 and 2000 ($1.95\% \text{ yr}^{-1}$) were replaced by losses between 2000
120 and 2016 ($2.11\% \text{ yr}^{-1}$) in southern Kenya. In the Watamu-Malindi region, a shallow reef system lost
121 77% of its seagrass in 30 years (Fig. 1), with rates of loss increasing from $0.73\% \text{ yr}^{-1}$ (1986-2000) to
122 $4.64\% \text{ yr}^{-1}$ (2000-2016). Seagrass cover increased in Gazi ($0.95\% \text{ yr}^{-1}$) and Vanga ($0.34\% \text{ yr}^{-1}$) Bays
123 between 1986 and 2000, then declined at $1.68\% \text{ yr}^{-1}$ and $1.8\% \text{ yr}^{-1}$, respectively. Pate Island suffered
124 the largest total decline (Fig. 1), losing 40.09 km^2 ($1.5\% \text{ yr}^{-1}$) between 1986 and 2016.

125 S2-derived mapping accuracy from the field points was 73% (total), 76.7% (emergent), and 69.3%
126 (submerged); we assume this is indicative for the whole region when estimating extent. Using the
127 Landsat image overlap method, we estimated accuracies of 67.8%, 82.6%, and 82.8% for the 1986,
128 2000, and 2016 maps respectively. Emergent classification accuracy was also higher across all images
129 (85.65%) compared to the submerged zones (80.03%).

130 Maximum total C loss from seagrass was 21.15% of the original over 30 years (Table 1). Total C_{org}
131 loss was estimated to be $0.07 \text{ Tg C yr}^{-1}$ using the regional estimate [3]; the global mean [10] gives an
132 estimate of $0.05 \text{ Tg C yr}^{-1}$. The 2000-2016 acceleration in decline implied loss rates of $0.12 \text{ Tg C yr}^{-1}$
133 and $0.07 \text{ Tg C yr}^{-1}$ for the regional and global estimates, respectively. Total estimated C loss was 2.17
134 Tg over 30 years.

135 **Table 1** Estimates of total C_{org} in Kenyan seagrass meadows

Year	Regional Carbon Estimate (Tg C) ¹	Global Carbon Estimate (Tg C) ²
1986	10.28	7.16
2000	9.95	6.95
2016	8.11	5.78

136 ¹ based on [3], ² based on [10].

137 Discussion and Conclusions

138 The last published estimate of seagrass coverage for Kenya is 112.39 km² [12], potentially
 139 underestimating the total area by 204.7 km². Estimating total C from Kenyan seagrass using [10] and
 140 [12] gives 1.89 Tg, whereas our estimate of seagrass coverage and C_{org} from [3] gives 7.65 Tg C. If
 141 these figures are representative of Africa, global analyses of C storage in seagrass meadows are
 142 significantly underestimating the contribution from this region.

143 The rate of loss of seagrass in Kenya is below the global estimate of 7% yr⁻¹ [1]. Patterns of loss vary
 144 between the north and south, with some regions (e.g. Malindi) showing more pronounced change.
 145 Slower rates of loss in Kenya may reflect historically low population sizes and industrialisation.
 146 Kenyan population growth is ~ 2.9% yr⁻¹ and is faster along the coast and in urban areas [13,14]; this
 147 driver probably underpins the accelerating rate of loss. Seagrass decline is often caused directly by
 148 fishing pressures and urban development and indirectly by eutrophication and climate change [15].
 149 In sites such as Gazi Bay, we found numerous geometrical scars indicating fishing damage to
 150 seagrass meadows; anecdotal information suggests this occurs along the southern Kenya coast.
 151 Seagrass loss in the north may be related to destruction of mangroves for large-scale irrigation,
 152 aquaculture and rice paddies [16,17] leading to sedimentation, thus reducing the area of seabed
 153 suitable for seagrasses. Because turbidity may prevent the detection of seagrass using remote
 154 sensing, our approach may not be as useful in areas with sporadically high turbidity if this occurs in
 155 the images used.

156 Promoting sustainable fishing practices, non-destructive land-use and communicating the
157 importance of seagrass habitats should be at the forefront of management strategies. The role of
158 seagrass as nurseries for fish has immediate traction for fishing communities, whilst including
159 seagrass C in payments for ecosystem services schemes, such as that already operating for
160 mangroves in Kenya [18] may bring new opportunities for conservation funds. African seagrass
161 remains poorly researched; if these results are representative then global estimates of seagrass
162 coverage and C stocks are underestimates

163 Ethics

164 There were no ethical issues relevant to this research.

165 Data Accessibility

166 Supporting datasets have been uploaded to the Dryad repository [10], doi:
167 <https://doi.org/10.5061/dryad.n08qs2s>.

168 Competing Interests

169 We have no competing interests.

170 Author Contributions

171 WDH, RB, and MH conceived the initial project. WDH analysed the satellite imagery and produced
172 the results with the help of RB and MH. MH helped conduct the field survey. All authors wrote the
173 final manuscript. All authors agree to be held accountable for the content therein and approve the
174 final version of the manuscript.

175 Acknowledgements

176 We thank Ankje Frouws, Caroline Wanjiru, Peter Musembi, Tom Peter Kisiengo and Laitani Suleimani
177 for their help in collecting groundtruthing data, staff at KMFRI Gazi for organisation and the people
178 of Gazi for hosting.

179 Funding

180 This work was funded by a grant from the British Council Newton Fund, grant no. 275670159.

181 References

- 182 1. Waycott M *et al.* 2009 Accelerating loss of seagrasses across the globe threatens coastal
183 ecosystems. *Proc. Natl. Acad. Sci.* **106**, 12377–12381. (doi:10.1073/pnas.0905620106)
- 184 2. Githaiga MN, Gilpin L, Kairo JG, Huxham M. 2016 Biomass and productivity of seagrasses in
185 Africa. *Bot. Mar.* **59**. (doi:10.1515/bot-2015-0075)
- 186 3. Githaiga MN, Kairo JG, Gilpin L, Huxham M. 2017 Carbon storage in the seagrass meadows of
187 Gazi Bay, Kenya. *PLoS One* **12**. (doi:10.1371/journal.pone.0177001)
- 188 4. Hedley JD, Harborne AR, Mumby PJ. 2005 Simple and robust removal of sun glint for mapping
189 shallow-water benthos. *Int. J. Remote Sens.* **26**, 2107–2112.
190 (doi:10.1080/01431160500034086)
- 191 5. Hochberg EJ, Atkinson MJ, Andréfouët S. 2003 Spectral reflectance of coral reef bottom-types
192 worldwide and implications for coral reef remote sensing. *Remote Sens. Environ.* **85**, 159–
193 173. (doi:10.1016/S0034-4257(02)00201-8)
- 194 6. Stumpf RP, Holderied K, Sinclair M. 2003 Determination of water depth with high-resolution
195 satellite imagery over variable bottom types. *Limnology Oceanogr.* **48**, 547–556.
196 (doi:10.4319/lo.2003.48.1_part_2.0547)

- 197 7. McIntyre K, McLaren K, Prospere K. 2018 Mapping shallow nearshore benthic features in a
198 Caribbean marine-protected area: assessing the efficacy of using different data types
199 (hydroacoustic versus satellite images) and classification techniques. *Int. J. Remote Sens.* **39**,
200 1117–1150. (doi:10.1080/01431161.2017.1395924)
- 201 8. Phinn SR, Roelfsema CM, Mumby PJ. 2012 Multi-scale, object-based image analysis for
202 mapping geomorphic and ecological zones on coral reefs. *Int. J. Remote Sens.* **33**, 3768–3797.
203 (doi:10.1080/01431161.2011.633122)
- 204 9. Harcourt WD, Briers RA, Huxham M. Data from: The Thin(ning) Green Line? Mapping Kenya's
205 Seagrass. Dryad Digital Repository. (doi:10.5061/dryad.n08qs2s)
- 206 10. Fourqurean JW *et al.* 2012 Seagrass ecosystems as a globally significant carbon stock. *Nat.*
207 *Geosci.* **5**, 505–509. (doi:10.1038/ngeo1477)
- 208 11. Githaiga MN. 2016 The role of seagrass meadows in Gazi Bay, Kenya as carbon sinks.
209 Edinburgh Napier.
- 210 12. Short, T F. 2005 Global distribution of seagrasses. *UNEP World Conserv. Monit. Cent. - Mar.*
211 *metadata Cat.* , 13–15.
- 212 13. Kenya 2014, Demographic and Health Survey.
213 <https://dhsprogram.com/pubs/pdf/fr308/fr308.pdf>
- 214 14. Linard C, Kabaria CW, Gilbert M, Tatem AJ, Gaughan AE, Stevens FR, Sorichetta A, Noor AM,
215 Snow RW. 2017 Modelling changing population distributions: an example of the Kenyan
216 Coast, 1979–2009. *Int. J. Digit. Earth* **10**, 1017–1029. (doi:10.1080/17538947.2016.1275829)
- 217 15. Orth RJ *et al.* 2006 A Global Crisis for Seagrass Ecosystems. *Bioscience* **56**, 987–996.
218 (doi:10.1641/0006-3568(2006)56[987:agcfse]2.0.co;2)
- 219 16. Kirui KB, Kairo JG, Bosire J, Viergever KM, Rudra S, Huxham M, Briers R a. 2013 Mapping of

220 mangrove forest land cover change along the Kenya coastline using Landsat imagery. *Ocean*
221 *Coast. Manag.* **83**, 19–24. (doi:10.1016/j.ocecoaman.2011.12.004)

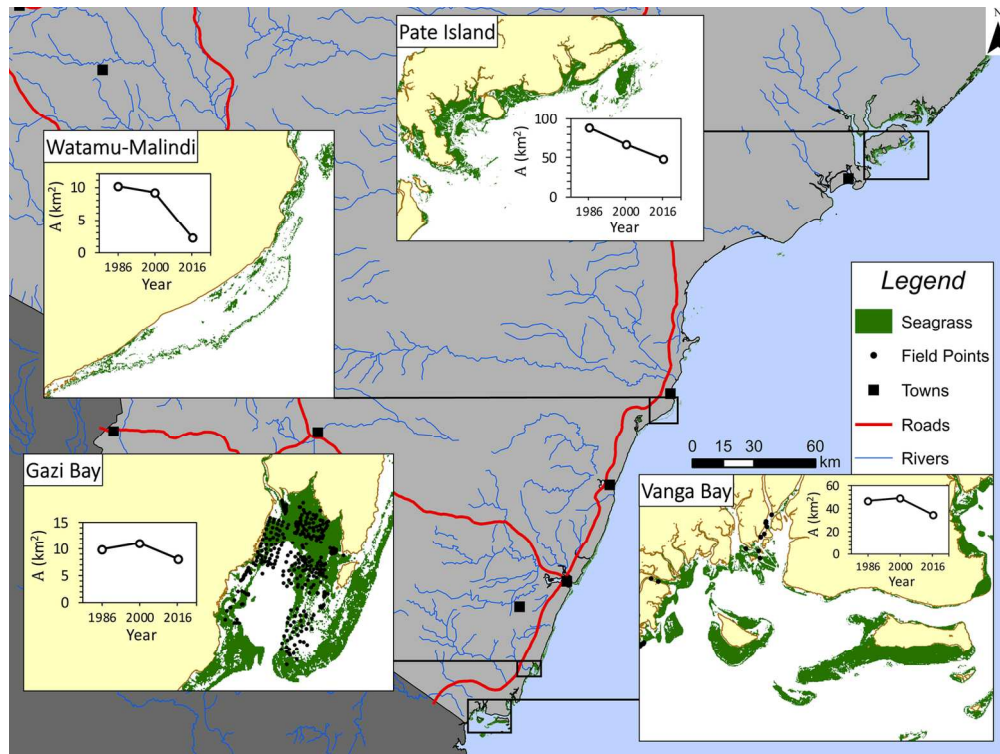
222 17. Abuodha PAW, Kairo JG. 2001 Human-induced stresses on mangrove swamps along the
223 Kenyan coast. *Hydrobiologia* **458**, 255–265.

224 18. Huxham M, Emerton L, Kairo J, Munyi F, Abdirizak H, Muriuki T, Nunan F, Briers R a. 2015
225 Applying Climate Compatible Development and economic valuation to coastal management:
226 A case study of Kenya's mangrove forests. *J. Environ. Manage.* **157**, 168–181.
227 (doi:10.1016/j.jenvman.2015.04.018)

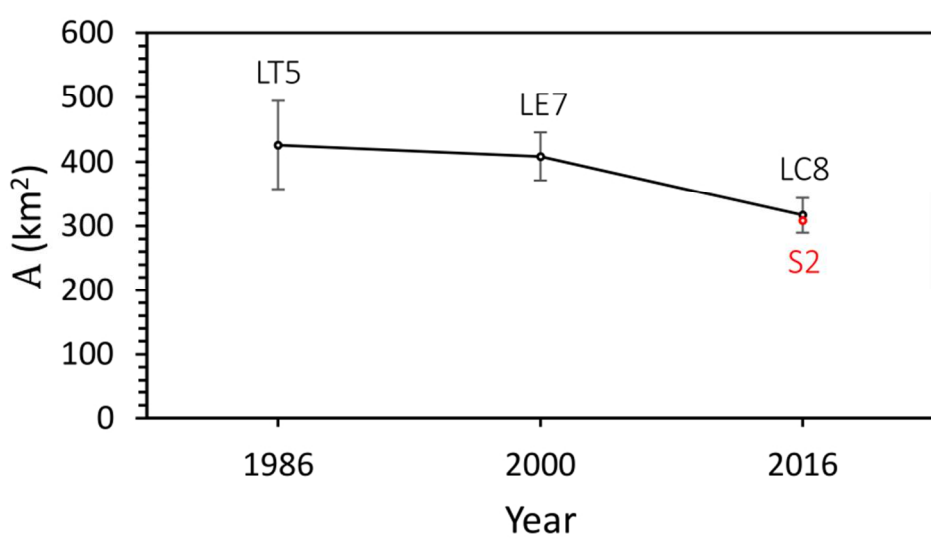
228 Figure Captions

229 Fig. 1 Seagrass coverage in Kenya. Inset panels display LC8 derived maps and temporal records for
230 representative sites.

231 Fig. 2 Changes in Kenyan seagrass coverage 1986 to 2016 using Landsat (black) and S2 (red). Error
232 bars were calculated by multiplying the % residual accuracy by total coverage to give a \pm range.



139x104mm (300 x 300 DPI)



333x194mm (72 x 72 DPI)

View Only